SOCIETY OF ACTUARIES

LIVING to 100
SOCIETY OF ACTUARIES INTERNATIONAL SYMPOSIUM

Mortality and Longevity

Aging and Retirement

The Mathematical Mechanism of Biological Aging

January 2020

The Mathematical Mechanism of Biological Aging

AUTHOR

Boquan Cheng
University of Western Ontario

Bruce Leonard Jones, FSA, FCIA, Ph.D.
University of Western Ontario

Xiaoming Liu, Ph. D.
University of Western Ontario

Jiandong Ren, Ph.D.
University of Western Ontario

SPONSOR

Society of Actuaries:
Aging and Retirement Research
Committee on Life Insurance Research
Financial Reporting Section
Mortality and Longevity Research
Product Development Section

The Mathematical Mechanism of Biological Aging

Boquan Cheng, Bruce Jones, Xiaoming Liu and Jiandong Ren
Department of Statistical and Actuarial Sciences
University of Western Ontario
London, ON, N6A 5B7 Canada

March 4, 2020

Abstract

Despite aging being a universal and ever-present biological phenomenon, describing this aging mechanism in accurate mathematical terms — in particular, how to model the aging pattern and quantify the aging rate — has been an unsolved challenge for centuries. In this paper, we propose a class of Coxian-type Markovian models which can provide a quantitative description of the well-known aging characteristics – the genetically determined, progressive and essentially irreversible process. Our model has a unique structure, including a constant transition rate for the aging process, and a functional form for the relationship between aging and death with a shape parameter to capture the biologically deteriorating effect due to aging. The force of moving from one state to another in the Markovian process indicates the intrinsic biological aging force. The associated increasing exiting rate captures the external force of stress due to mortality risk on a living organism.

The idea of the paper is developed from Lin and Liu (2007). A big difference is that, in this paper, our model uses a functional form for model parameters, which allows a parsimonious yet flexible representation for various aging patterns. Our proposed mathematical framework can be used to classify the aging pattern and the key parameters of the model can be used to measure and compare how human aging evolves over time and across populations.

1 Introduction

Human life is a very personal affair. It is your life and mine and that of our neighbor. Each life is a separate and distinct entity; yet there is a common stamp upon all... Many lives are cut short...; an accident or an acute illness may snuff out the light before it is burned out. But burn out it will, ultimately, even if no such

accidents intervene.
L.I. Dublin et al. (1949)

In the above sentence, Dublin et al. (1949) have well described the fact that, while individual lifetimes could have been affected by many personal and random factors, there is this ubiquitous aging process underneath the life of all human beings.

Then, what is "aging"?

To begin with, let us quote the definition of "aging" from Jones (1956): *Aging, as applied to living organisms, is the genetically determined, progressive, and essentially irreversible diminution with the passage of time of the ability of an organism or of one of its parts to adapt to its environment, manifested as diminution of its capacity to withstand the stresses to which it is subjected (i.e. the increase of susceptibility to certain diseases with age), and culminating in the death of the organism.*

Jones' definition has provided some characteristics about the aging process: such as genetically determined, progressive and essentially irreversible. But it was unclear on what capacities and how they decline with the passage of time in this aging definition. Like much other research at that time (before the middle of the 20th century), the studies on aging process were mainly descriptive and not accessible for measurement due to the lack of directly observable aging-related data. For this reason, the earlier theories of aging tried to associate the impact of aging with the increasing death rates as a way to justify their hypothesis quantitatively. In other words, it was a common practice in the past that the exponentially increasing mortality pattern (e.g., the Gompertz law of mortality, due to its good fit to a large portion of adult mortality rates) acted as a manifest of the "indirectly" observed aging process[1]

However, we would like to clarify the relationship between aging and death: While the mortality rate is strongly correlated to the rate of aging, the two are not exactly equivalent. There are many external factors that can cause pre-mature death, and/or even alter the aging process. To name a few, these factors include (but not limited): family background, education, income, lifestyle, marital status, accidents, acute diseases, and so on. According to Herskind et al. (1995), an additive genetic component explains about 2 percent of variability in life span, indicating non-genetic factors make substantial contribution to life span. Rather than thinking of aging and death in terms of the cause and effect relationship, it is now believed that the age-pattern of mortality risk results from interaction between the process of individual aging and external stresses, as stated in Yashin et al. (2012) and many references therein.

[1]As a matter of fact, many researchers in the demographic and actuarial fields considered the Gompertz mortality law to be the first one based on biological arguments, and in Gompertz's 1872 paper, he 'endeavored to enquire if there could be any physical cause for the consistent patterns of death among people', see Olshansky and Carnes (1997).

Another big change in the past few decades regarding the studies of aging is that many researchers began to collect longitudinal data of aging-related factors. These factors include body mass index, diastolic blood pressure, pulse pressure, pulse rate, level of blood glucose, hematocrit and serum cholesterol; again see Yashin et al. (2012) and references therein for the recent research in this direction. Different from many previous studies, the observations in these studies are obtained from young healthy individuals in order to understand how the biological processes develop in aging humans even before the onset of chronic diseases. In Yashin et al. (2012), it is found that different factors display different average age patterns and different dynamic properties. Some factors follow monotonic changes with increasing age; some are non-monotonic (e.g., increase then decline). Their findings also reveal that, when an individual's physiological indices deviate from their "optimal" values, one will experience higher-than-average mortality risk. From our perspective, their research might be more useful in understanding why some individuals can live longer life than others. However, if we want to develop a holistic quantitative tool to describe the aging effect of population, we might need to work on more general statistics.

By more general statistics, we mean concepts similar to allostatic load defined in Crimmins et al. (2003) or the biomarker as defined in Belsky et al. (2015). In summary, these are compiled indices based on various physiological functions across multiple organ systems (e.g., pulmonary, periodontal, cardiovascular, renal, hepatic, and immune function), to measure the cumulative biological burden developed over time or to mark the deterioration degree of an aging body. Despite the intensified studies in the past few decades and better longitudinal data accessibility now, the research in this area is still in its infant stage. This is largely due to the complexity of the living and dying process. From our point of view, it seems impossible to reach a commonly accepted biological aging index in the near future.

As a result, instead of taking an absolute approach in which one needs to select one or multiple representative aging indices, we propose a class of Coxian-type Markovian models which can provide a quantitative description of the well-known aging characteristics—"the genetically determined, progressive and essentially irreversible" process. Our model has a unique structure, including a constant transition rate for the aging process, and a functional form for the relationship of aging and death with a shape parameter to capture the biologically deteriorating effect due to aging. The proposed model incorporates two separate yet related forces in this Markovian framework: the force of aging (i.e., the intrinsic biological process) and the force of dying (i.e., the external forces from environmental stress including accidents, accessibility of nutrition and medical care, etc).

The idea of the paper is developed from Lin and Liu (2007). A big difference is that, in this paper, our model uses a functional form for model parameters, which allows a parsimonious yet flexible representation for various aging patterns. In addition, the lifetime distribution resulting from the proposed model should not be treated as a mortality model. Rather, the proposed model allows the modeller to take into account

the death probabilities associated with aging, which plays an inseparable and inevitable role to the ending of all lives.

The proposed model belongs to a big class of distributions — the so-called phase-type distribution. There is a long history of using phase-type distributions for survival modelling in the category of "absorbing time" distributions; see Aalen (1995), Asmussen et al. (1996), Lin and Liu (2007), Su and Sherris (2012), to list a few. Phase-type distributions can be clearly implemented when the states of the underlying process are observable and can be pre-specified. Otherwise, the flexibility of phase-type distributions might turn into a disadvantage since it will make model estimation much more difficult due to the non-uniqueness property of the phase-type distribution (Slud and Suntornchost, 2014). Our defined aging process is a latent process; however, a carefully designed functional form for model parameters helps mitigate the non-identifiability problem.

Our proposed mathematical framework can be used to specify the aging pattern and the key parameters of the model can be used to measure the deterioration effect of aging. Our model can also provide biologically meaningful comparisons regarding how human aging evolves over time and across populations. Other advantages of the model include that

- The model has a small number of parameters that can be conveniently estimated using maximum likelihood estimation. The parsimonious structure of the model ensures that the model can be uniquely identified with a given data set and the resulting model can provide a meaningful biological interpretation.
- The model is flexible in terms of how it represents the impact of aging on mortality.
- The model introduces randomness associated with aging and allows for quantifiable heterogeneity in terms of the physiological age of individuals in a population.
- This heterogeneity allows one to capture mortality selection at older ages, that is, the tendency for less healthy lives of a given age to experience higher mortality, leaving a healthier group of survivors.

These features of the model make it useful for a variety of actuarial applications. For example, in life insurance, the model can be used in the analysis of the impact of anti-selective lapsation on mortality experience. In life or health insurance, an extended version of the model, as in Govorun et al. (2018), can be used to determine premium adjustments based on information collected during the underwriting process.

The paper is organized as follows. In Section 2, we introduce our phase-type aging model. We begin with some background on phase-type distributions followed by the characteristics of a subclass known as Coxian phase-type distributions. We then introduce our model, which is a special case of the latter, and describe

the parametric structure of the model. In Section 3, we discuss how it can be calibrated using lifetime data. We illustrate these ideas using a small data set providing lifetimes of residents of a retirement community. In Section 4, we present some further analysis of our model. We illustrate how it can reproduce the lifetime distribution of a very different aging model. Through a simulation study, we show the challenge in estimating the number of model states with only lifetime data and demonstrate how the number of states influences the variability in how individuals age according to the model. Section 5 concludes the paper with a summary and some suggestions for further research.

2 The Proposed Phase-Type Aging Model (PTAM)

2.1 Basic mathematics for phase-type distributions

In this section, we provide the definition of phase-type distribution and describe its basic properties. We have also tried to organize the material to facilitate discussion about the challenges in using this type of model in practice. For the general theory of phase-type distributions, see, for example, Neuts (1982) and Asmussen (1989).

Definition *Let Y_t be a time-homogeneous Markov process defined on a finite state-space $S = E \cup \Delta = \{1, 2, \cdots, m\} \cup \Delta$, where Δ is absorbing and the states in E are transient. Let Y_t have initial distribution $(\boldsymbol{\alpha}^\top, 0)$ (written as a row vector), and infinitesimal generator*

$$\begin{pmatrix} \boldsymbol{\Lambda} & \boldsymbol{q} \\ \mathbf{0} & 0 \end{pmatrix} \tag{2.1}$$

where $\boldsymbol{q} = -\boldsymbol{\Lambda}\boldsymbol{e}$ and $\boldsymbol{e}$ is the column vector of ones.

Let T denote the time until absorption or the time until death in the human lifetime context. Then T is said to follow a phase-type (PH) distribution with representation $(\boldsymbol{\alpha}, \boldsymbol{\Lambda})$.

One very intriguing aspect of phase-type models is the intuitive interpretation that they provide about the underlying biological/engineering mechanism of the system which results in the lifetime survival distribution. In plain language, the survival time of such a system is the sum of the sojourn times in all states that the process has ever visited before it is absorbed. The survival probability at any time t is the total probability that the process is in any state other than the absorbing state at time t.

For $s \geq 0, t \geq 0,\ i, j \in E$, let $P_{ij}(s, s+t)$ be the transition probability from state i to state j during the

time period $(s, s+t]$:

$$P_{ij}(s, s+t) = \Pr(Y_{s+t} = j | Y_s = i)\,. \tag{2.2}$$

Because Y_t is a time-homogeneous Markov process, the probability $P_{ij}(s, s+t)$ does not depend on s, so we write $P_{ij}(t) = P_{ij}(s, s+t)$ for all $s \geq 0$.

Denote $\boldsymbol{P}(t) = \{P_{ij}(t)\}_{i,j\in E}$ as the transition probability matrix (among the transient states) of Y_t in the time interval $[0, t]$. Then it satisfies the Kolmogorov forward equation,

$$\frac{d}{dt}\boldsymbol{P}(t) = \boldsymbol{P}(t)\boldsymbol{\Lambda}\,, \tag{2.3}$$

with the initial condition $\boldsymbol{P}(0) = \boldsymbol{I}$, where $\boldsymbol{I}$ is the identity matrix.

The Kolmogorov forward equation has the unique solution

$$\boldsymbol{P}(t) = \exp(\boldsymbol{\Lambda} t), \tag{2.4}$$

where the matrix-exponential $\exp(\boldsymbol{\Lambda} t)$ is defined by

$$\exp(\boldsymbol{\Lambda} t) = \sum_{n=0}^{\infty} \frac{t^n}{n!}\boldsymbol{\Lambda}^n.$$

As a result, the survival function of the time until absorption random variable T can be expressed as

$$S(t) = \boldsymbol{\alpha}^\top \exp(\boldsymbol{\Lambda} t)\boldsymbol{e}, \quad t > 0\,. \tag{2.5}$$

Notice that the ith element of the vector

$$\mathbf{p}(t) = \boldsymbol{\alpha}^\top \exp(\boldsymbol{\Lambda} t) \tag{2.6}$$

gives the probability that $Y_t = i$, and $\mathbf{p}(t)\boldsymbol{e}$ gives the probability that $Y_t \in E$.

Phase type distributions have simple matrix expressions for their survival function, probability density function, Laplace transform and raw moments. Furthermore, the class of phase-type distributions is dense in the space of all continuous positive distributions. That is, any distribution on $(0, \infty)$ can, at least in principle, be approximated closely by a phase-type distribution. Therefore, it has been successfully applied in many areas to obtain explicit analytical solutions. However, obtaining numerical results by solving differential equations (2.4) or calculating matrix exponential (2.5) is not trivial, especially when the dimension of the matrix $\boldsymbol{\Lambda}$ (i.e. the number of states, m) is big.

In addition, a general phase type distribution has many parameters, and sometimes, the way of parameterizing a model is not unique (Asmussen et al., 1996). Therefore, the parameter estimation of phase-type distributions is known to be difficult. As discussed in the later part of this paper, the problem of non-uniqueness

in parameter specification is usually intermingled with estimation difficulties of the model, especially when the model contains a large number of states and the model parameters are close to each other.

We remark that this paper considers the application of phase type modelling to the aging process, similar to Aalen (1995), Lin and Liu (2007), and Su and Sherris (2012). In such applications, the model may involve a large number of states but the intensity matrix is sparse and follows certain structure.

2.2 Coxian phase-type distributions

In the following, we discuss the Coxian-type distribution, which is a special type of phase-type distribution with initial distribution $\boldsymbol{\alpha}^\top = (1, 0, \cdots, 0)$ and intensity matrix

$$\boldsymbol{\Lambda} = \begin{bmatrix} -(\lambda_1 + h_1) & \lambda_1 & & & \\ & -(\lambda_2 + h_2) & \lambda_2 & & \\ & & \ddots & & \\ & & & -(\lambda_{i-1} + h_{m-1}) & \lambda_{i-1} \\ & & & & -h_m \end{bmatrix}, \tag{2.7}$$

where $\lambda_i > 0$ and $h_i > 0$ for all $i \in E$. The Coxian model is illustrated in Figure 1. Since the process only starts from state 1, the survival function of the Coxian-type model only depends on the first row of the transition matrix $\boldsymbol{P}(t)$, which is denoted by $\mathbf{p}_1(t)$. Let the kth element of $\mathbf{p}_1(t)$ be denoted as $P_{1k}(t)$ or simply $P_k(t)$.

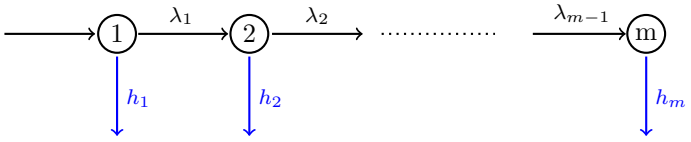

Figure 1: Diagram for a Coxian-type Markovian process

Then the Kolmogorov forward equation is given by

$$\begin{cases} \frac{dP_1(t)}{dt} & = -(\lambda_1 + h_1)P_1(t); \\ \frac{dP_k(t)}{dt} & = \lambda_{k-1}P_{k-1}(t) - (\lambda_k + h_k)P_k(t), \ k = 2, 3..., m. \end{cases} \tag{2.8}$$

Obviously $P_1(t) = e^{-(\lambda_1 + h_1)t}$. In addition, $P_k(t)$ for $k = 2, ..., m$ can be obtained iteratively, yielding

$$P_k(t) = \sum_{j=1}^{k} \frac{(-1)^{k-1}\lambda_1 ... \lambda_{k-1}}{\prod_{s=1, s\neq j}^{k}(\lambda_j + h_j - \lambda_s - h_s)} e^{-(\lambda_j + h_j)t}, \ k = 2, ..., m. \tag{2.9}$$

Finally, the survival function of T is given by

$$S(t) = \sum_{k=1}^{m} P_k(t). \tag{2.10}$$

When the dimension of the Coxian model is small and the parameter values are far apart so that the denominator of (2.9) is not too small, equation (2.9) may be used to quickly evaluate the distribution. However, in lifetime modelling, the model to be used may contain a large number of states with λ_is and h_is being very close to each other. Using (2.9) causes numerical problems because the values of each term in summation are large and have alternative signs.

2.3 A class of Coxian phase-type distributions - our proposed PTAM

The Coxian distribution provides a natural and appealing approach to modeling aging. Unfortunately, the general Coxian distribution has many parameters, making estimation difficult. We can greatly simplify the model while retaining considerable flexibility by imposing some structure. That is, we can specify mathematical forms for the pattern of λ_i values, representing the internal force of aging, and the pattern of h_i values, representing the external force of dying. If the mathematical functions used for this involve a small number of parameters, then our estimation task becomes manageable.

First assume that the number of states (physiological ages) m in our model is known. We will address how to determine m later in the paper.

Now assume that $\lambda_i = \lambda$, a constant, for all $i = 1, 2, \ldots, m-1$. In doing so, we are assuming that the aging rate is uniform over time, so that the rate of increase in physiological age is uniform. This makes some sense because calendar age increases uniformly. Although our assumed aging rate is constant, there is variability in transition times. Therefore, at any calendar age, an individual may be in a number of different states representing different physiological ages. This is the same idea used by Lin and Liu (2007) in which the aging-related transition intensity parameter is specified as a constant. To capture the complete age-specific mortality pattern, Lin and Liu (2007) allowed λ_i to vary so that non-aging-related mortality causes can be accommodated. However, in our model, we focus on aging. Given this focus, our model is most applicable at human ages beyond the attainment of adulthood.

The value of λ needs to be appropriate to the value of m. We need the rate of progression through the states to be large enough that some individuals will reach state m, or there is no need to have as many as m states. However, we want only a small proportion of individuals to survive to state m. We therefore let

$$\lambda = m/\psi, \tag{2.11}$$

where ψ can be thought of as the life span of individuals in the population of interest. The parameter ψ need not be a limiting age, as there is no limiting age in our model. However, ψ should be a high age to which only a very small proportion of individuals will survive. This parameter can be estimated from data or chosen based on prior opinion. For human lifetimes, a value of ψ between 100 and 120 may be reasonable.

We next specify a form for the h_i values. First, suppose that h_1 and h_m are fixed. These are parameters to be estimated. We then require a smooth pattern of h_i values for i between 1 and m. We achieve this by letting

$$h_i^s = \frac{m-i}{m-1}h_1^s + \frac{i-1}{m-1}h_m^s.$$

In other words, powers of h_i are obtained as a linear interpolation between the corresponding powers of h_1 and h_m. We then have

$$h_i = \left(\frac{m-i}{m-1}h_1^s + \frac{i-1}{m-1}h_m^s\right)^{1/s}.$$

We can use this for any real s except $s = 0$, when the expression is undefined. However, the limiting case as $s \to 0$ gives

$$h_i = h_1^{\frac{m-i}{m-1}}\, h_m^{\frac{i-1}{m-1}}.$$

In this case, $\log h_i$ is obtained as a linear interpolation between $\log h_1$ and $\log h_m$. Thus, the parameter s can take any real value. Then, for $i = 1, 2, \ldots, m$,

$$h_i = \begin{cases} \left(\frac{m-i}{m-1}h_1^s + \frac{i-1}{m-1}h_m^s\right)^{1/s} & s \neq 0, \\ h_1^{\frac{m-i}{m-1}}\, h_m^{\frac{i-1}{m-1}} & s = 0. \end{cases} \tag{2.12}$$

This structure is reminiscent of the well-known Box-Cox transformation introduced by Box and Cox (1964).

Note that, when $s = 1$, we have a linear pattern of h_i values with increasing i. When $s = 0$ we have an exponential pattern of h_i values. Furthermore, when $s < 1$, the pattern will be convex, and when $s > 1$, the pattern will be concave. Figure 2 shows the patterns of h_i values for $s = 0$, 1 and 2. For human aging, we would expect that $s = 0$ is the most appropriate of the three values. The value that one actually uses may be estimated from lifetime data.

In summary, we propose a Coxian distribution with five parameters to be specified: m, ψ, h_1, h_m and s. We may be able to choose m and ψ based on prior knowledge, or a combination of lifetime data and prior knowledge. Having established the values of m and ψ, λ is determined from (2.11), and h_1, h_m and s are easily estimated from lifetime data.

Ideally, our aging model would be calibrated using aging-related data, rather than just lifetime data. In other words, if observations of one or more key aging variables are taken at one or more times while each individual is alive in addition to ages at death, we could estimate the model parameters with less uncertainty. Govorun et al. (2018) describe a method of doing this. However, it is beyond the scope of this paper.

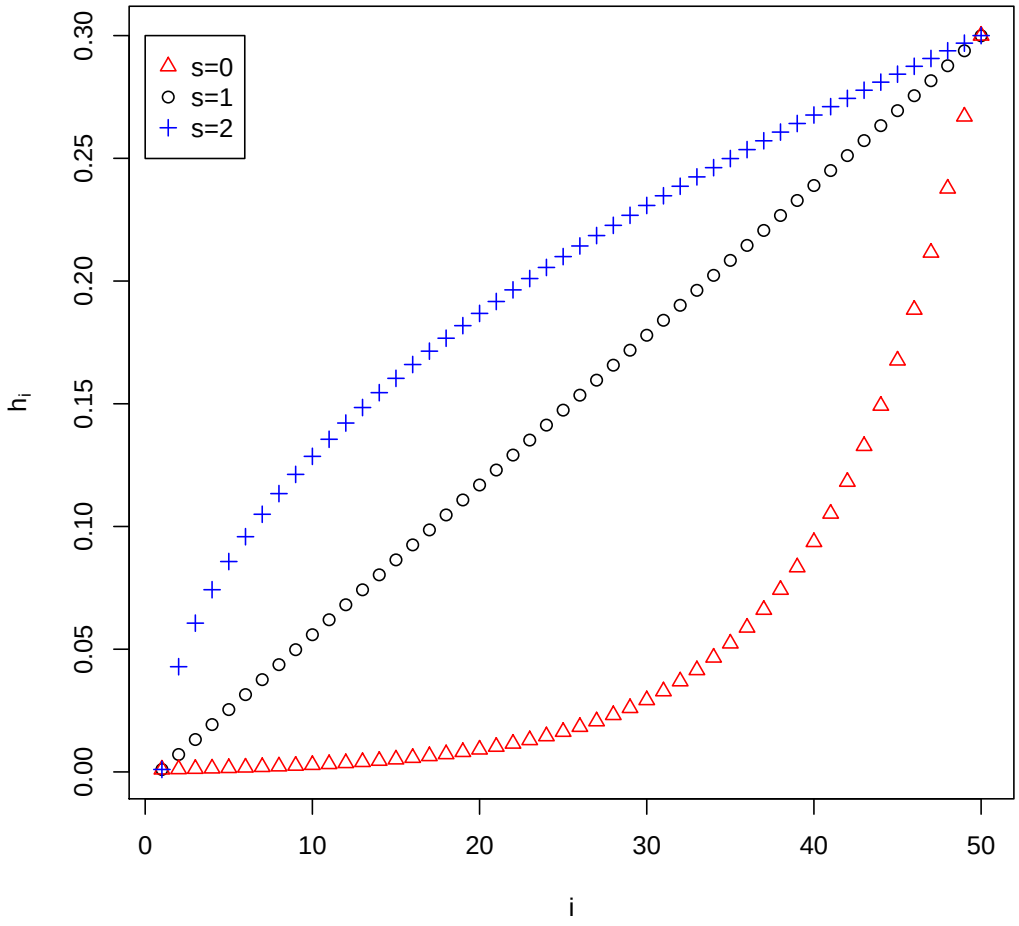

Figure 2: Values of h_i determined using $h_1 = 0.001$, $h_m = 0.3$ and $s = 0$, 1 and 2.

3 Model Estimation and Application

3.1 Parameter estimation

The parameters in our model can be estimated using maximum likelihood estimation, which we now describe.

Suppose that $\boldsymbol{\theta}$ is the parameter vector we wish to estimate. If we have chosen values of m and ψ, then $\boldsymbol{\theta}= (h_1, h_m, s)$. Further, suppose we wish to estimate this parameter vector using data on lifetimes only. Specifically, for each observed individual $j = 1, \ldots, n$ we observe (ℓ_j, t_j, δ_j), where ℓ_j is the age at which individual j entered observation, t_j is the age at which individual j left observation, and $\delta_j = 1$ if individual j died at time t_j and $\delta_j = 0$ otherwise.

The likelihood function is given by

$$L(\boldsymbol{\theta}) = \prod_{j=1}^{n} \frac{f(t_j;\boldsymbol{\theta})^{\delta_j}\, S(t_j;\boldsymbol{\theta})^{1-\delta_j}}{S(\ell_j;\boldsymbol{\theta})}, \tag{3.13}$$

where $S(t;\boldsymbol{\theta})$ is our model survival function, and $f(t;\boldsymbol{\theta})$ is our model probability density function. Recall that we have

$$S(t;\boldsymbol{\theta}) = \boldsymbol{\alpha}^{\top} \exp(\Lambda t)\, \mathbf{e},$$

and

$$f(t;\boldsymbol{\theta}) = \boldsymbol{\alpha}^{\top} \exp(\Lambda t)\, \mathbf{q}.$$

Both Λ and $\mathbf{q}$ are functions of $\boldsymbol{\theta}$. Therefore, for a given $\boldsymbol{\theta}$, we can calculate the value of the likelihood or the loglikelihood, $l(\boldsymbol{\theta}) = \log L(\boldsymbol{\theta})$. The loglikelihood can then be maximized numerically with respect to $\boldsymbol{\theta}$ to obtain the maximum likelihood estimates.

3.2 Application using data from a retirement community

To illustrate how our aging model can be calibrated using lifetime data, we consider data from Channing House, a retirement community in Palo Alto, California. The data set includes the entry age and age at death (or study end) for 462 people (97 males and 365 females) who resided in the facility between January 1964 and July 1975. These residents were covered by a health care program, which provided easy access to care at no cost. This may have resulted in lower than average mortality. For the purpose of this paper, we decided to fit our aging model to the female data only, i.e. a data set on a relatively small group of homogeneous individuals — all females living in the same community with the same access to health care and, very likely, similar lifestyles, as well as a similar socio-economic status. This is not ideal, but this is the best we can do to ensure all other variables that are likely to affect death are as similar as possible among these individuals, and the only variable that we cannot control is the underlying aging process.

Only 362 of the 365 female records were kept, because three records had equal entry and exit ages. Of the 362 females, 130 died while in the community, and the other 232 survived until the end of the observation period. The youngest entry age was just over age 61, and the oldest exit age was just under age 101. So the data pertain to aging over this age range.

Since our model assumes all individuals start in state 1, but we expect some variability in state by age 61, we assume for this example that the aging process starts at age 50. Also, we assume, somewhat arbitrarily, that age 105 is the end of the life span. This meets our condition that it be a high age to which only a very small proportion of individuals will survive. In fact, nobody in our small sample of females were observed to live older than this age. Therefore, $\psi = 105 - 50 = 55$. Also, based on experience, we believe that $m = 100$ aging

states is appropriate for modeling aging above age 50. We discuss in more detail the principles we use to specify m and ψ later in the paper. With $m = 100$ have that $\lambda = m/\psi = 100/55 = 1.8182$. Using maximum likelihood estimation as described above, we obtain $\widehat{h}_1 = 0.00175471$, $\widehat{h}_m = 1.27518$ and $\widehat{s} = -0.0734710$. The parameter estimators are highly correlated and the variances are large. This is not at all surprising, as the data set is very small. With a larger data set, we would have less uncertainty about the parameter estimates. However, the estimates seem reasonable and lead to a good fit to the data.

The estimates of h_i that result from $\widehat{h}_1$, $\widehat{h}_m$ and $\widehat{s}$ are shown in Figure 3. The pattern of values look reasonable given that they represent instantaneous mortality rates that apply between ages 50 and 105.

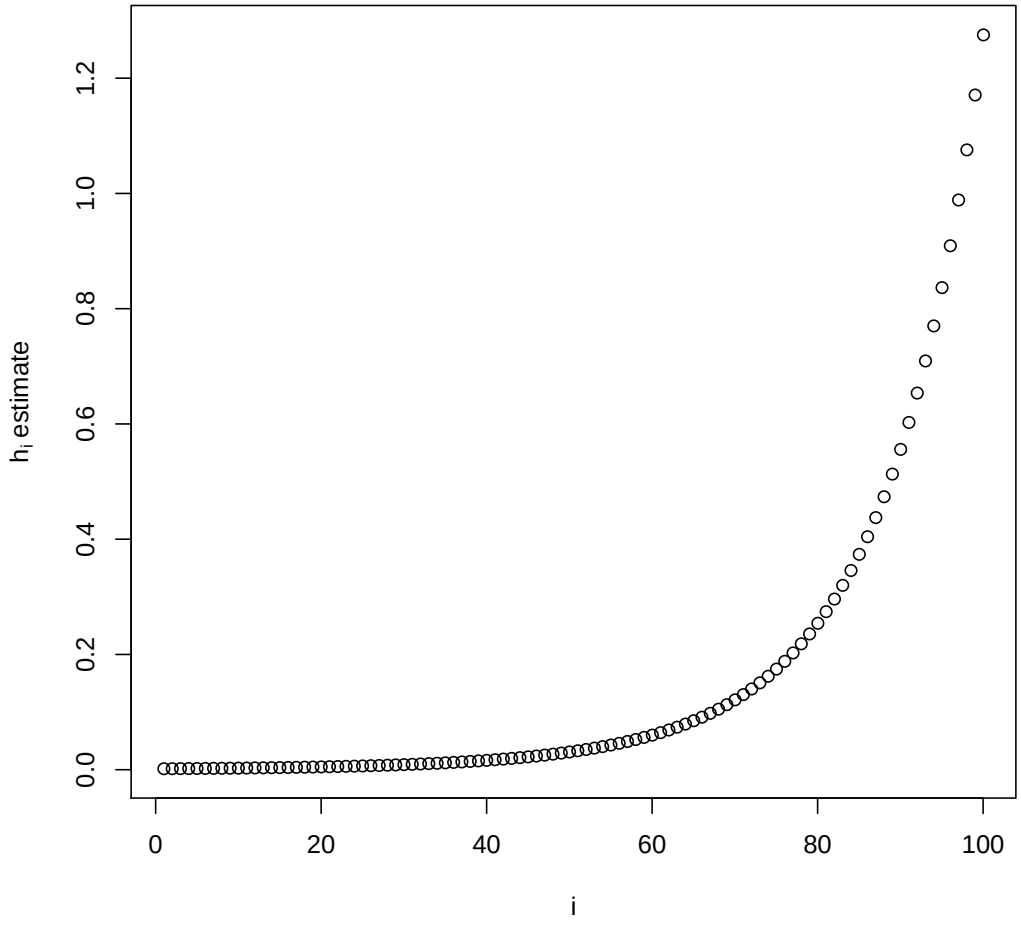

Figure 3: Estimates of h_i obtained by calibrating the PTAM model using the Channing House female data.

Figure 4 shows the force of mortality and the log (base 10) of the force of mortality based on the fitted model. Once again the behavior is quite reasonable.

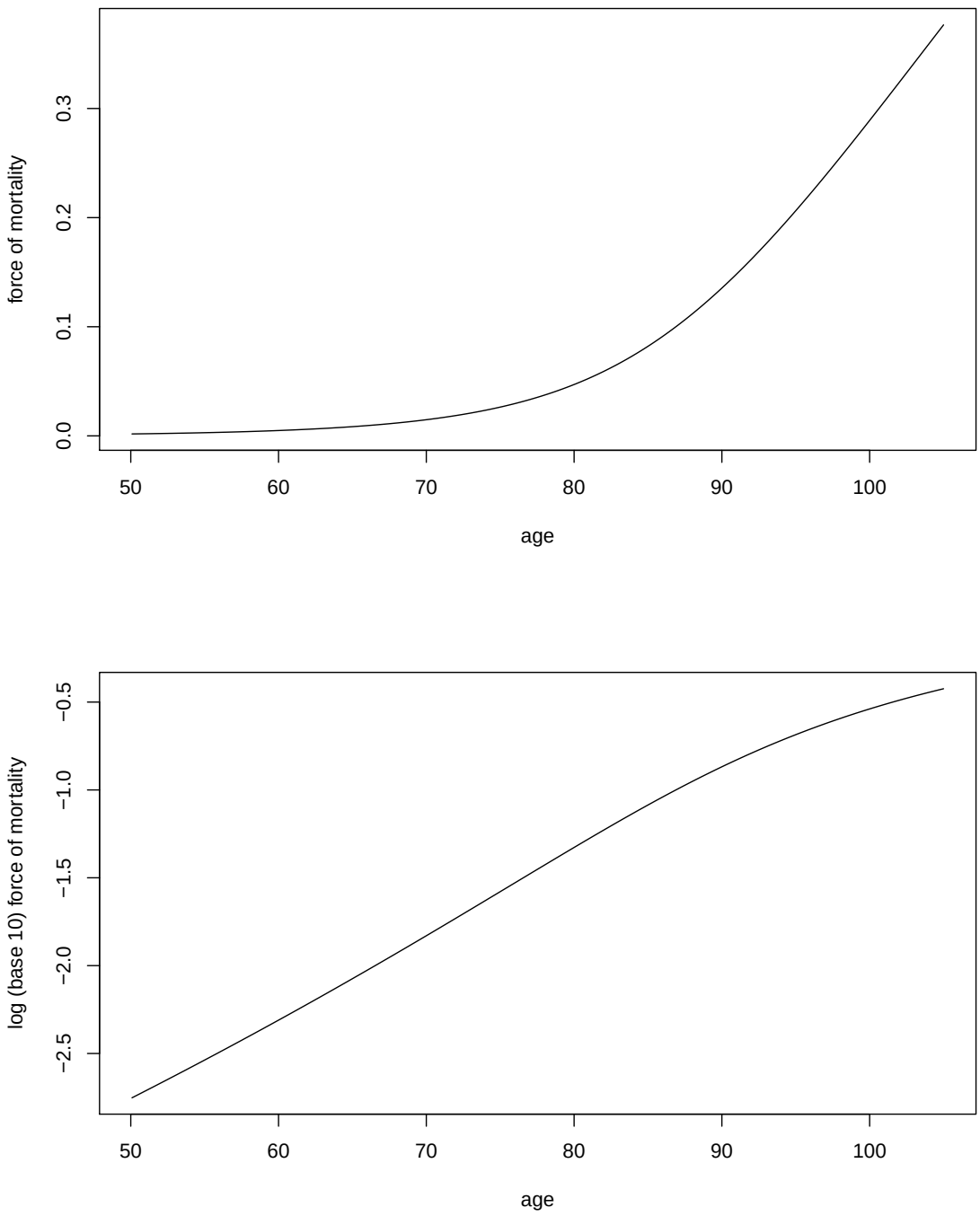

Figure 4: Force of mortality and log (base 10) force of mortality based on the PTAM model calibrated using the Channing House female data.

In Figure 5 we illustrate the goodness of fit of our model to the Channing House data by plotting the fitted survival function along with the Kaplan-Meier nonparametric survival function estimates. We observe that our model fits quite well – and our fitted model estimates stay within the 95 percent confidence limits based on the Kaplan-Meier estimator.

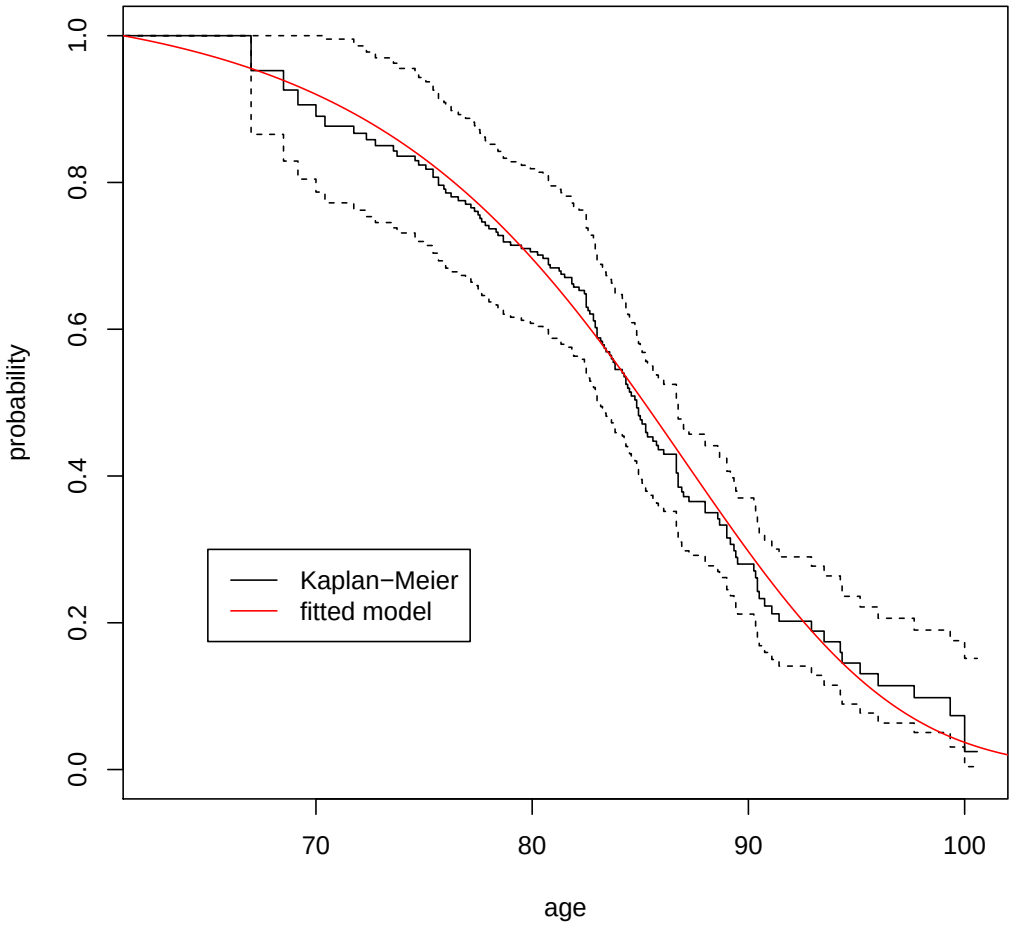

Figure 5: Survival function based on the PTAM model calibrated using the Channing House female data, along with the Kaplan-Meier estimates of the survival function and corresponding 95 percent confidence limits (dashed).

With our fitted model, we can perform a variety of analyses of the aging process. For example, it is interesting to examine the distribution of the state of an individual at different ages, given that the individual is alive at these ages. The probabilities of associated with this distribution, that is $\Pr(Y_t = i | Y_t \in E)$, are given by the vector

$$\mathbf{p}(t)/\mathbf{p}(t)\mathbf{e},$$

where $\mathbf{p}(t)$ can be calculated using equation (2.6). Since these probabilities correspond to age $50+t$ in our example, it is intuitively appealing to transform the state Y_t to a comparable value that we can interpret as the individual's physiological age. Let

$$\text{Phyiological age at calendar age } t = 50 + \frac{Y_t - 1}{m-1}\,\psi. \tag{3.14}$$

Then an individual in state 1 has physiological age 50, and an individual in state 100 has physiological age $50 + \frac{100-1}{99}(55) = 105$. We can now determine the distribution of physiological age at any calendar age.

Figure 6 shows the distribution of physiological age at ages 60, 70, 80 and 90 for the PTAM model calibrated using the Channing House female data. We observe that the physiological age distribution has less variability at younger ages. This is mainly due the fact that we started the process at age 50, so that the all individuals have physiological age 50 at age 50. At older ages, the variability stabilizes. We also observe that the mean physiological age, indicated by the vertical lines, is very close to 60 at age 60. However, at older ages, the mean physiological age becomes noticeably smaller than the age. This is due to mortality selection - individuals with a higher physiological age have a higher mortality rate. Therefore, survivors tend to be those with a lower physiological age.

We can gain further insight into our aging model by observing how the paths of the process behave. We can do this by simulating several paths and plotting them. To simulate a path, we assume that the individual is in state 1 (physiological age 50) at age 50. The individual will stay in state 1 for a length of time that is exponentially distributed with rate $\lambda + h_1$. We can generate this exponential random variable. At the end of the stay in state 1, the individual will die with probability $h_1/(\lambda + h_1)$ and move to state 2 with probability $\lambda/(\lambda + h_1)$. We can generate a uniform (0,1) random variable to determine whether or not the individual dies at this time. If not, we generate the time spent in state 2 (exponential with rate $\lambda + h_2$) and continue until the individual dies.

We simulated ten paths of the process and plotted them in Figure 7. Once again the state of the process has been transformed to physiological age as described above. The figure illustrates once again the variability in physiological age at different ages, but also shows the extent to which individual paths depart from uniform aging over time. That is, we observe the "wigglyness" of individual paths.

4 Further Analysis of our Proposed PTAM

Our basic modelling principle is that the (length of) life is the result of two important forces: the force of aging (i.e., the intrinsic biological process) and the force of dying (i.e., the external forces from environmental stress including accidents, accessibility of nutrition and medical care, etc). In addition, we want to model

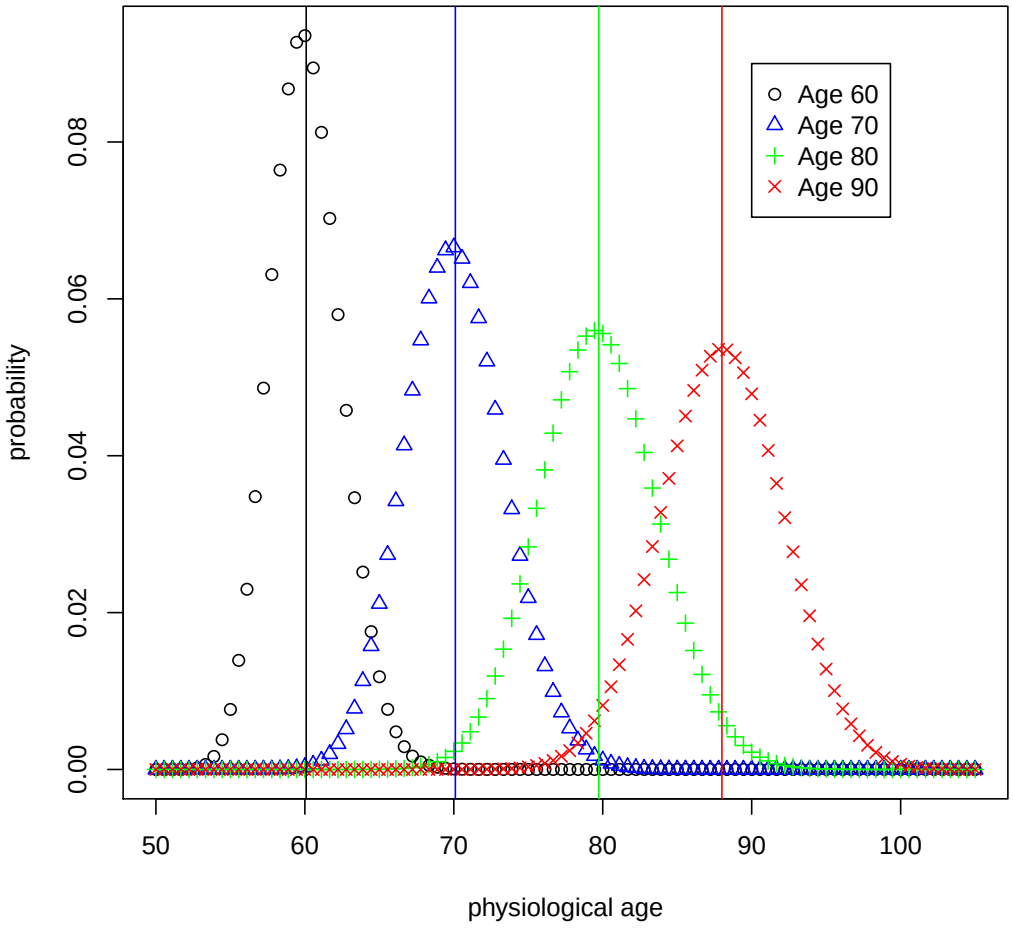

Figure 6: Physiological age distribution at ages 60, 70, 80 and 90 based on the PTAM model calibrated using the Channing House female data. Vertical lines indicate the means of the distributions

the two forces using a **stochastic** approach; specifically, we adopt the Markovian model framework of the Coxian distribution. That is, we define a finite number of states representing different physiological capacity levels and transition intensities determining the rate of progression through the states. These states (with labelling suitably transformed) are interpreted as an individual's physiological age, since they are used to classify an individual's physiological capacity at the moment. As a result, we have naturally incorporated the concept of heterogeneity into the lifetime dynamic process by introducing the so-called "*physiological age*".

We mentioned in Section 1 that, since the middle of the 20th century, many researchers have begun to collect longitudinal data on various physiological variables. The most striking finding may be the fact that

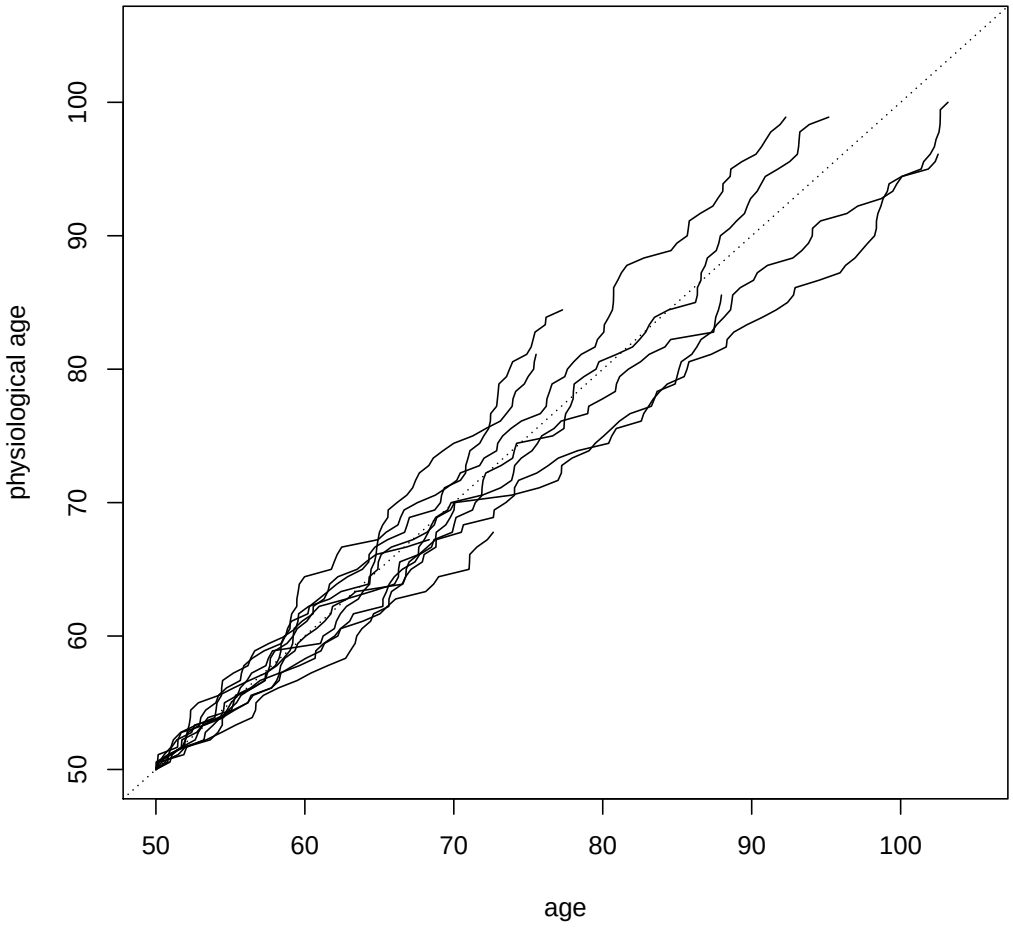

Figure 7: Ten simulated paths from age 50 until death based on the PTAM model calibrated using the Channing House female data.

the decline of these physiological functions as a result of the underlying aging process follows a slow, uniform and roughly linear pattern with age. This suggests that, according to our assumption of a uniform rate of increase in physiological age, declines in physiological function are decreasing, approximately linear, functions of physiological age.

Notwithstanding the appeal of our approach, other strategies can be used to construct a Coxian distribution. We discuss one of these below and illustrate that our model is nearly equivalent in terms of the resulting lifetime distribution.

4.1 The Le Bras dual linear Markovian model

We now describe a model developed by Szilard (1959) and Le Bras (1976). Szilard (1959) proposes an aging process theory. It assumes that chromosomes mutate with constant rate in cells. If a cell accumulates too many mutations, it will cease functioning. Once a certain percentage of cells stop functioning in a human body, the body will die. Furthermore, Le Bras added an assumption that the inherited chromosomal mutation in the human body follows a Markov process. For a newborn, each cell mutates with rate λ_0 initially. Then new mutations occur with additional rate $i\lambda$, proportional to the total number of mutations i that have happened in this cell, and each cell dies with rate $i\mu$, proportional to i as well. Hence, let state i of a Markov process represent the state in which cells have accumulated i mutations in total. Then the transition rate from state i to $i+1$ is $\lambda_0 + i\lambda$ and the transition rate from state i to the absorbing state, i.e. to death, is $i\mu$.

Figure 8: Diagram for the Le Bras dual linear model

The Le Bras model has been discussed by Yashin et al. (1994) in the following form: $\lambda_i = \lambda_0 + i\lambda$ and $\mu_i = \mu_0 + i\mu$, where μ_0 is the initial exiting rate. See Figure 8 for the diagram of the model. Here, the Le Bras model has an infinite number of states. Following the steps in section 2, one can derive the transition probability

$$P_i(t) = \frac{e^{-(\mu_0+\lambda_0)t}}{i!}\left(\frac{\lambda(1-e^{-(\lambda+\mu)t})}{\lambda+\mu}\right)^i \prod_{k=1}^{i}\left(\frac{\lambda_0}{\lambda}+k-1\right). \tag{4.15}$$

Recognizing that $P_i(t)$ follows a binomial series pattern, it can be verified that

$$S(t) = \sum_{i=0}^{\infty} P_i(t) = e^{-(\lambda_0+\mu_0)t}\left(\frac{\lambda+\mu}{\mu+\lambda e^{-(\lambda+\mu)t}}\right)^{\frac{\lambda_0}{\lambda}} \tag{4.16}$$

The Le Bras model is one of the first few attempts that have successfully incorporated physical/biological assumptions in a mathematical framework. Hence, it is important to review their approach, as this can help us to gain insight on how our proposed model can be useful.

More remarks about the Markovian approach and the Le Bras model:

- Under the further assumption that $\mu \ll \lambda$, the hazard function of the Le Bras model can be approxi-

mated by

$$\mu(t) = \left(\mu_0 - \frac{\mu\lambda_0}{\lambda}\right) + \frac{\mu\lambda_0}{\lambda}\, e^{(\lambda+\mu)t},$$

which is equivalent to the 3-parameter Gompertz-Makeham mortality model, $\mu(t) = a + be^{ct}$, with

$$a = \mu_0 - \frac{\mu\lambda_0}{\lambda}, \quad b = \frac{\mu\lambda_0}{\lambda}, \quad c = \lambda + \mu\,.$$

See Yashin et al. (1994) for further details. The important contribution of the Le Bras model is the dual linear structure in describing the aging process (the linear pattern for λ_i) and the deteriorating effect (the linear pattern for μ_i) that could result in a Gompertz form of exponentially increase mortality pattern.

- In Yashin et al. (1994), the authors discuss the Le Bras model. It was found that, starting from a fixed frailty assumption, it is possible to derive the same mortality model. Hence, it was argued that, in the statistical analysis of data, results and conclusions depend not only on the data but also on basic assumptions about the mechanism which generated the data. In other words, in reality, the use of lifetime data alone is not sufficient to distinguish between different mechanisms generating the observed mortality patterns. More sophisticated data need to be used to validate the assumption.

- There are some similarities between the Le Bras model and our proposed model. The most interesting similarities are that 1). both models differentiate the aging effect from the aging process, and 2). both use a Coxian structure to describe the interaction between the intrinsic force of aging and the external force of dying. However, from a practical perspective, the Le Bras model seems too restrictive in the sense that it requires a dual-linear pattern in its parametric form, which cannot be tested or modified.

For all of these reasons, we prefer our model structure to that of Le Bras model.

4.2 A simulation study

We are interested in examining if our PTAM model can capture the probabilistic features of the Le Bras model.

To explore this, we simulated 5,000 lifetime observations from the Le Bras model with the parameters given in Table 1. We then fit our model to the simulated data. Before estimating the other parameters using the MLE method, we determine a reasonable value of the life span parameter, ψ. Once again, ψ is a high age to which only a very small proportion of individuals will survive. Since we have 5,000 complete lifetimes, we set ψ as follows:

$$\psi = \widehat{\mathrm{TVaR}}_{0.999}(T), \tag{4.17}$$

where $\widehat{\text{TVaR}}_{1-\alpha}(T)$ is an empirical estimate of $\text{TVaR}_{1-\alpha}(T)$, obtained from the simulated data. Since our simulated sample size is 5,000, $\widehat{\text{TVaR}}_{0.999}(T)$ is the average of the five largest observations. We obtain $\psi = \widehat{\text{TVaR}}_{0.999}(T) = 112.55$. We estimate the remaining parameters using the MLE method. Figure 9 shows a histogram of the simulated data, the probability density function (pdf) of the Le Bras model and the pdf of the fitted PTAM model. The MLE of m is determined by fitting the model for different but fixed m using the MLE method, and comparing their respective Negative Log-Likelihood (NLL) values. As one can see in Table 2, when $m = 225$, we obtain the lowest NLL value.

Table 1: Parameters value

	λ_0	λ	μ_0	μ
The Le Bras model	0.6	0.07	0.001	0.4×10^{-4}
Our fitted PTAM model	h_1	h_m	λ	s
with $m = 225$	0.0008	1.65349	1.99908	-0.11118

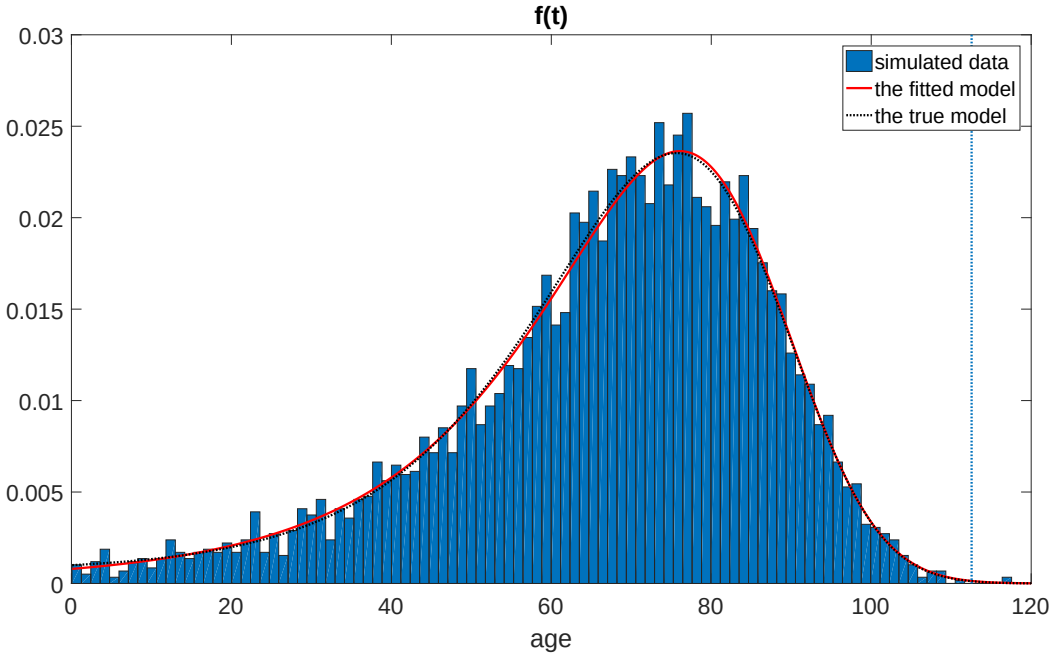

Figure 9: Histogram of 5,000 lifetimes simulated from the Le Bras Model. The fitted model with m=225 is plotted along with the true model. The dotted vertical line indicates the location of $\psi = 112.55$.

Figure 9 shows that if the observed mortality rates are truly generated from the Le Bras model, our model can provide a nearly equivalent representation. We are able to achieve the same goodness of fit as the Le Bras model by allowing the exiting rate h_i to increase faster than linearly. The fact that s can be flexible to take any value in order to accommodate the data (in this example $s = -0.11118$) is a specific feature of our model.

Hence, we have found an alternative to the Le Bras dual linear model with constant transition rate λ, though our model has a slightly different interpretation of the underlying aging mechanism. While the original Le Bras model contains an infinite number of the states, our PTAM model re-labels them into m states. The aging process is still modelled as marching forward from one state to the next, and the impact of aging is still described as increased frailty to hazard with higher indexed state. The only difference is the way of labeling the states. Transforming from the Le Bras model to our PTAM model, the earlier states may need to be split into more states, while the later states may need to be grouped, but not in a linear fashion. The overall effect is that, in our model framework, the transitions from one to another are required to occur evenly due to the use of the constant transition rate λ. Correspondingly, the pattern for h_i changes from a linear increase to a pattern that has to climb slightly faster than exponentially, as indicated by the parameter s taking a small negative value.

In Table 2, we show additional results from fitting our model to the simulated data. As required, the estimate of the parameter λ increases with m. We have also plotted the survival functions, density functions and hazard functions of these fitted models with m ranging from 200 to 250 in Figure 10, the dotted vertical line indicates the location of $\psi = 112.55$. For ages up to this value, the distributions are very close to each other. However, for the hazard functions, there are small but noticeable differences beginning near age 100.

NLL	h_1	h_m	λ	s	m	$\min(\lambda + h_1, h_m)$
21631.884	0.00081	2.00325	1.77637	-0.12373	200	1.77718
21631.826	0.0008	1.83922	1.86518	-0.11829	210	1.83922
21631.806	0.0008	1.70795	1.95400	-0.11336	220	1.70795
21631.713	0.0008	1.65349	1.99908	-0.11118	225	1.65349
21631.813	0.00079	1.60064	2.04282	-0.10886	230	1.60064
21631.843	0.00078	1.51076	2.13164	-0.10469	240	1.51076
21631.889	0.00078	1.43544	2.22046	-0.10089	250	1.43544

Table 2: Estimation results using different m based on 5,000 lifetimes simulated from the Le Bras limit distribution. The first column gives the negative log-likelihood - NLL. The last column is the limit of the resulting hazard function $h(t)$ as $t \to \infty$.

Looking more carefully at the hazard functions in the bottom left panel of Figure 10, we find that the fit doesn't change symmetrically as m moves away from its optimal value. The model with $m = 250$ fits much better than the one with $m = 200$. Also, the model with $m = 250$ gives the highest hazard rate at the right end of the life span. For phase-type distributions, it is a well-known property that

$$\lim_{t\to\infty} h(t) = \min_{i=1,\cdots,m}\{d_1, d_2, \cdots, d_m\},$$

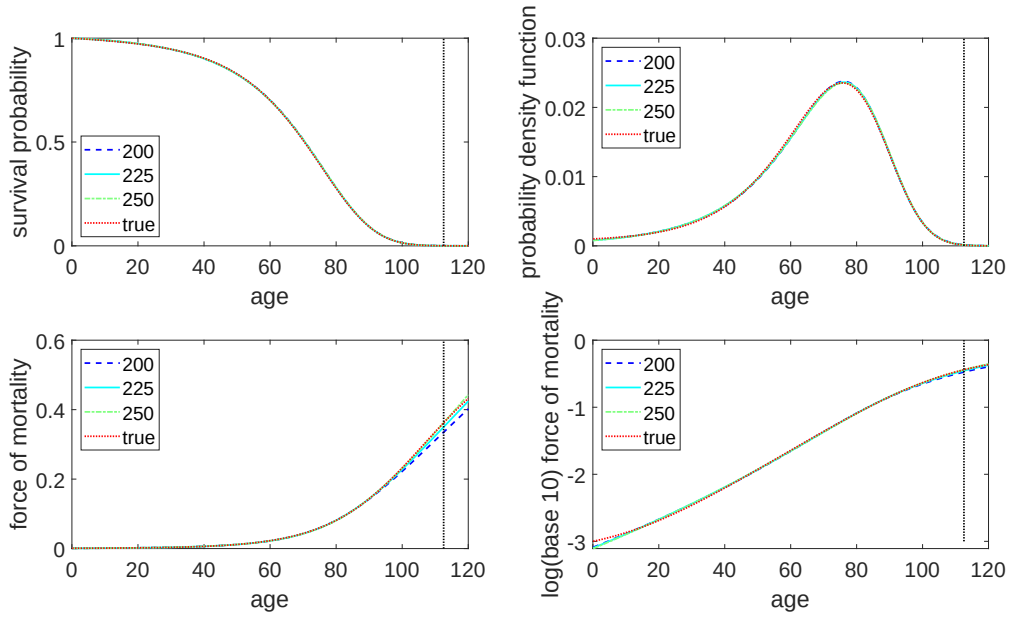

Figure 10: Fitted survival function - S(t), probability density function - f(t), hazard function - h(t), and log (base 10) hazard function. Each graph includes four curves corresponding to the fitted model with m=200, 225 and 250, as well as the true model. The dotted vertical line indicates the location of $\psi = 112.55$.

where the d_i's are the eigenvalues of the transition intensity matrix $\mathbf{\Lambda}$. In our PTAM model, we have

$$\lim_{t\to\infty} h(t) = \min\{\lambda + h_1, h_m\},$$

since the eigenvalues $\lambda + h_i$ increase except for the last element of the matrix $\mathbf{\Lambda}$. The limit of $h(t)$ for each fitted model is provided in the last column of Table 2, and the model with $m = 250$ has the lowest value of this limit.

In Figure 11, we show the logarithm of the hazard function of the fitted models from age 80 to 500. While the graph show interesting differences in tail behavior, these difference occur well beyond the age range that is relevant from a practical perspective.

The statistical equivalence of the outcome between two different model structures is of significant importance. By all means, what we propose here is a statistical model which focuses on describing the progressive and irreversible feature of the aging process. The interaction between aging and mortality is not the aging process itself, rather the aging effect which is subject to what we observe and how we observe it. In other words, the model aims at capturing the related increasing mortality phenomenon due to the aging process. It might be impossible to completely rule out some subjective element in how we perceive the process. The equivalence means that the interpretation of the internal aging process could be flexible depending on what and how we observe the process, but the model should be "true" to the ultimate observable facts—which is the observed

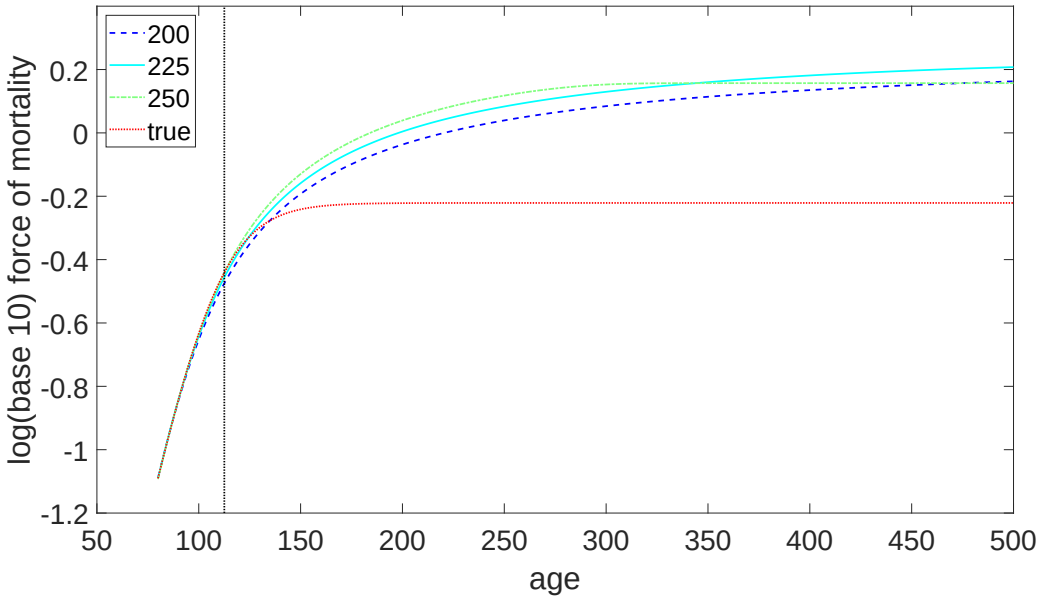

Figure 11: Fitted log (base 10) hazard function extended to age 500. Each graph includes four curves corresponding to the fitted model with m=200, 225 and 250, as well as the true model. The dotted vertical line indicates the location of $\psi = 112.55$.

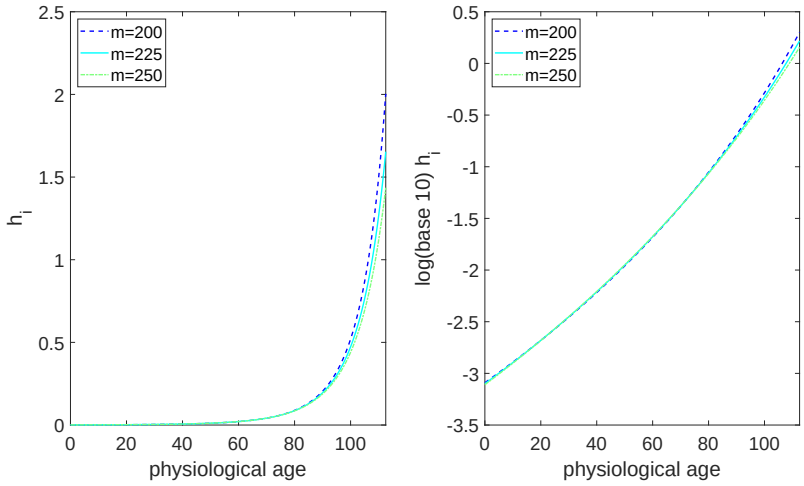

Figure 12: The left graph shows the exit rate h_i with m=200, 225 and 250. The right graph shows the log-exit rate with m=200, 225 and 250. Both are plotted against the physiological age $\frac{i-1}{m-1}\,\psi$.

death rates by age in this situation. This is the basic principle to validate a statistical model.

Now we move to another important concept that is introduced by our model framework. Similar to (3.14),

we can define a physiological age index based on our calibrated model:

$$\text{Physiological age index } X_t \text{ at calendar age } t = \frac{Y_t - 1}{m - 1}\,\psi. \tag{4.18}$$

So X_t is a random variable transformed from Y_t, and X_t can be interpreted as a physiological age index since it is associated with where an individual is at on the aging process. Note that X_t takes values from $[0, \psi]$. That is, X_t is not affected by the state number parameter m and has the same scale as the calendar age's upper limit ψ. This makes X_t a good counterpart for age t: for each individual which may follow a personalized aging process Y_t, there is this corresponding physiological age index X_t telling the health status of the individual at his/her calendar age t.

In Figure 12, we plot h_i versus the physiological age $\frac{i-1}{m-1}\,\psi$. The pattern of h_i on $[0, \psi]$ turns out to be quite stable with different m. This is another good feature of the proposed model, indicating that the underlying mechanism does not vary too much with m.

In our analysis so far, we have demonstrated that some key aspects of our aging model are quite stable with changing m. Our estimated value of m was determined by maximizing the likelihood. However, the likelihood is quite flat for values of m near the maximum. So there are only small differences in the lifetime distribution that result from different m. This leads to the question: How is the model affected by the value of m and how should m be determined?

While the lifetime distribution is relatively insensitive to m, the progression of physiological age with advancing calendar age is affected by m. In particular, the variability in physiological age is significantly affected by m. In fact, as $m \to \infty$, this variability disappears, and physiological age converges to calendar age. In particular, when m increases, the expected physiological age of an alive individual at calendar age $t \in (0, \psi)$ approaches t and the variability decreases. This phenomenon is illustrated in figure 13, where ten simulated sample paths for each of four different values of m: 25, 100, 225, and 1,000 are plotted. In fact, we hypothesize that with $m \to \infty$, $\mathbb{E}(X_t | Y_t \in E) = t$ and $Var(X_t | Y_t \in E) \to 0$.

Furthermore, the resulting hazard function takes on the behavior of our h_i values. That is, as m gets large, we observe that the hazard function, which is the expected exit rate, given by $h^m(t) = \mathbb{E}(h_{Y_t} | Y_t \in E)$ approaches

$$h(t) = \begin{cases} \left(\left(1 - \frac{t}{\psi}\right) h_1^s + \frac{t}{\psi} h_m^s\right)^{1/s} & s \neq 0, \\ h_1^{1-\frac{t}{\psi}}\, h_m^{\frac{t}{\psi}} & s = 0. \end{cases}$$

In addition, the variability of h_{Y_t} becomes smaller and smaller when m increases.

This is not surprising because of our observation in last paragraph that X_t approaches t when m goes to infinity.

Figure 13 shows ten simulated sample paths for each of four different values of m: 25, 100, 225, and 1,000. We observe that, as m increases, there is less variability in physiological age. And physiological age is converging to calendar age. This suggests that m should not be too large, or the model will not appropriately reflect the variability in physiological age. Obviously, m cannot be too small either, or there will too much variability in physiological age.

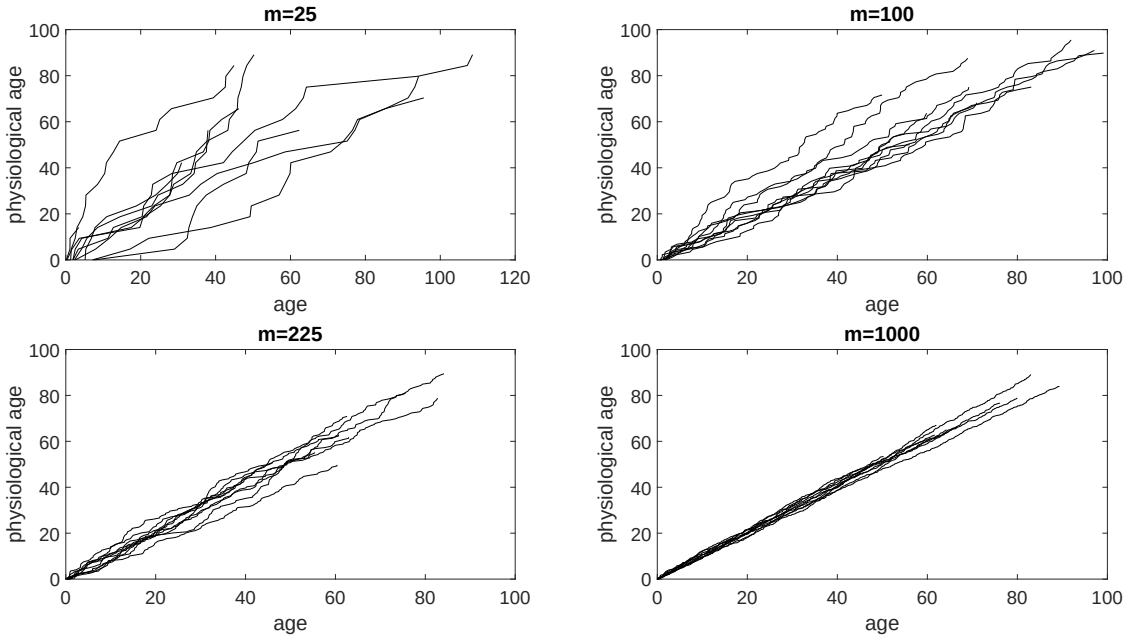

Figure 13: Ten simulated sample paths of the fitted PTAM model for each of four different values of m, holding the parameters h_1, h_m and s fixed.

In summary, we intend to choose m and ψ so that the calibrated model can reflect one's opinion about the variability in physiological age. Also since ψ tends to take a value close to the life span measured in years, the physiological age has a range between 0 and ψ, which seems to be a reasonable scale conversion from calender age. However, if one has data that includes information about one or more health variables related physiological age in addition to the lifetimes of individuals, then additional consideration can be given to estimating m and ψ along with the other parameters. This is the preferred approach if suitable data are available.

4.3 Comparing with the model in Lin and Liu (2007)

At last, it is worth comparing the proposed model in this paper with that in Lin and Liu (2007). According to our understanding, what Lin and Liu (2007) achieved is to demonstrate how the aging component, combined

Year	q	p	h_1	h_m	s
1811	9.3157e-09	3	1.71e-08	0.074532485	0.332803361
1861	2.6351e-13	5	8.52e-13	0.084431355	0.199403613
1911	1.8872e-15	6	5.14e-14	0.120627387	0.166163239

Table 3: Parameter q and p are values from Lin and Liu (2007), and their corresponding calibrated values in terms of our proposed form (2.12) for Swedish cohorts of year 1811, 1861, and 1911.

with other causes of death, can explain well the age pattern of mortality rates for observed cohorts. However, the main goal of this paper is not to reproduce mortality patterns; instead we aim at finding a way to describe the aging process, in which aging-related mortality rates are used to determine a quantitative measurement of the aging rate and the associated aging effect under our pre-defined model framework. Hence, the resulting lifetime distribution from our model cannot be treated as a mortality model as in Lin and Liu (2007).

In other words, our proposed functional form (2.12) can be used to replace the aging-related mortality rates in equation (3.3) in Lin and Liu (2007), which, for the convenience of readers, is provided below:

$$h_2(i) = i^p \cdot q$$

with parameter p and q estimated for three different cohorts.

We have matched our proposed functional form (2.12) to the three estimated patterns shown in Figure 5 of Lin and Liu (2007). The parameters of h_1, h_m and s for our model are given in Table 3 along with the values for q and p for the three cohorts from Lin and Liu (2007), respectively.

As shown in Figures (14) and (15), the functional form (2.12) can match three different scenarios in Lin and Liu (2007) perfectly well. The parameter s, which is supposed to capture the curvature of the death rates associated with aging process, ranges from 0.332803361 to 0.166163239 for cohorts born in 1811 to 1911. This appears to be a good feature of our proposed model. Compared with Lin and Liu (2007) in which the combinations of p and q are used to capture the aging-related mortality pattern in Figure 5 of the paper (also attached below—Figure (16)— for reader's convenience), here the parameter s can indicate well the meaning conveyed by using two parameters in Lin and Liu (2007).

5 Conclusions and future works

Research on the aging phenomenon has been intriguing for centuries, but the quantitative study of aging is still in its infancy due to the lack of directly observable aging-related data. For this reason, earlier theories

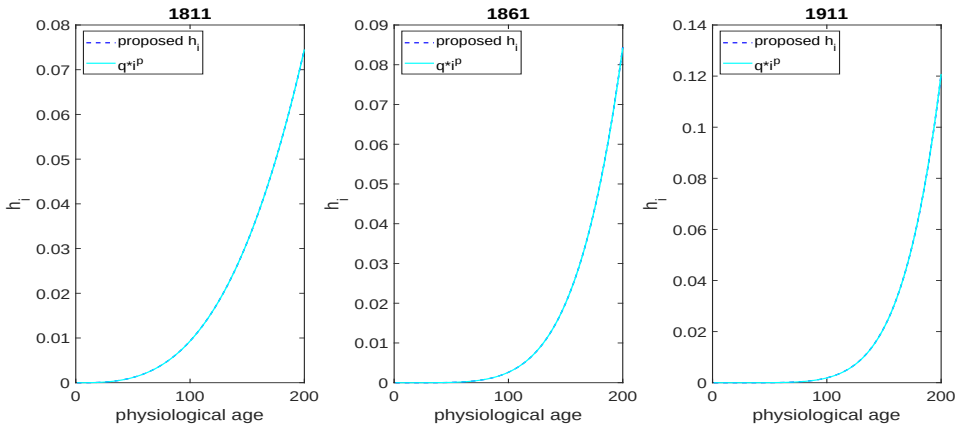

Figure 14: The calibrated h_i using the form (2.12) v.s. $h_i = i^p \cdot q$ in Lin and Liu (2007) for three cohorts.

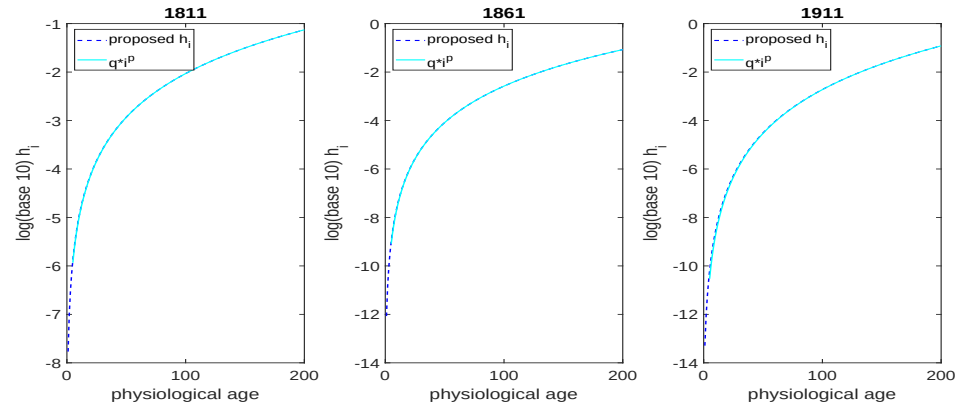

Figure 15: The calibrated h_i using the form (2.12) v.s. $h_i = i^p \cdot q$ in Lin and Liu (2007) for three cohorts.

of aging often use the impact of aging (e.g. the observed increasing death rates with age) to validate their underlying hypothesis about aging. As a result, many people automatically equate a model for aging to a model for mortality. Therefore, it is important to remark that our proposed model framework is an attempt to describe aging mechanism. Differentiating the aging effect from the aging process itself is a key contribution of our approach. Although we have used mortality rates by age to quantify the aging effect, any other aging-related variables can replace mortality rates if they are available. For example, medical expenditure was included as a covariate to enhance the aging profile in Govorun et al. (2018), which is a good example of how the current approach can be extended to incorporate other aging-related variables. In practice, the real challenge lies more in identifying proper aging-related variables and data availability, should the proposed model be adopted. At the same time, the observed increasing mortality rates at adult ages are still the best indicator for aging process nowadays, which is why we are using them in our aging model framework.

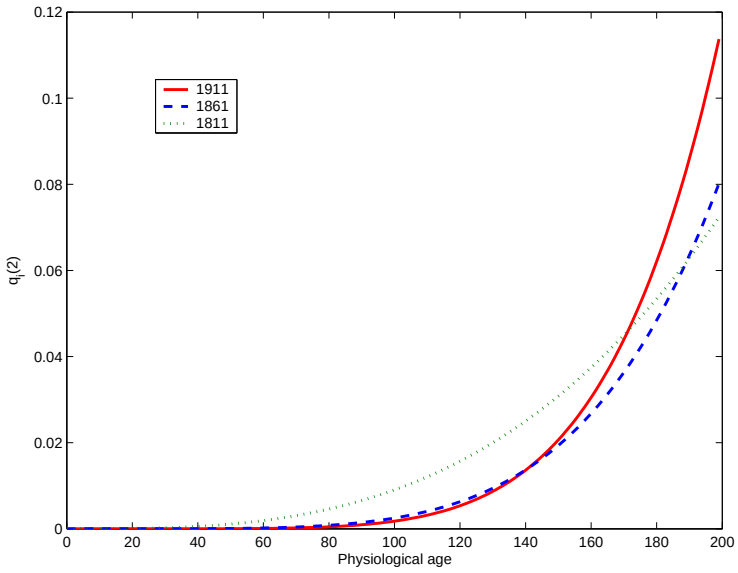

Figure 16: The original Figure 5 from Lin and Liu (2007).

So this paper has presented a mathematical model for aging. The model has a very natural interpretation, as individuals are assumed to age by progressing through a number of states, with a random time spent in each state. The model is made even more intuitive by transforming the state label to a scale that can be interpreted as physiological age (see Figure 12). As one would expect, the mortality rate increases as one moves from one state to the next, which is the consequence of aging. However, the force of aging and the force of mortality are separate components of the model.

We assume that the rate of aging is constant over time, so that individuals progress uniformly through the states. The pattern of state-specific mortality rates is determined using a three-parameter structure that allows considerable flexibility and includes linear and exponential patterns as special cases. Once the number of model states is specified, the rate of aging is determined so that individuals will reach the final state only very close to the end of the life span, which must be specified.

Our model can be calibrated with lifetime data using maximum likelihood estimation. However, in this case we have a lot of uncertainty about the estimate of the number of model states. This makes sense because the number of states determines the variability in physiological age. Since it is an aging model, it would obviously be better to calibrate it using data that has explicit information about aging - observed health-related variables.

One of the areas for future research is the exploration of methods for estimating parameters when data involve health observations as well as mortality information. The approach of Govorun et al. (2018) may work well.

Another area for future research involves investigating how to modify the model to allow for different populations or different birth cohorts. One option is to use different aging rates with mortality rates that are the same. Another is to allow the mortality rate parameters to be different.

Acknowledgment

The authors gratefully acknowledge financial support for this research through a grant from the Canadian Institute of Actuaries.

References

Aalen, O. O. (1995). Phase type distributions in survival analysis. *Scandinavian Journal of Statistics*, 22(4):447–463.

Asmussen, S. (1989). Exponential families generated by phase-type distributions and other markov lifetimes. *Scandinavian Journal of Statistics*, 16(4):319–334.

Asmussen, S., Nerman, O., and Olsson, M. (1996). Fitting phase-type distributions via the em algorithm. *Scandinavian Journal of Statistics*, 23(4):419–441.

Belsky, D. W., Caspi, A., Houts, R., Cohen, H. J., Corcoran, D. L., Danese, A., Harrington, H., Israel, S., Levine, M. E., Schaefer, J. D., et al. (2015). Quantification of biological aging in young adults. *Proceedings of the National Academy of Sciences*, 112(30):E4104–E4110.

Box, G. E. and Cox, D. R. (1964). An analysis of transformations. *Journal of the Royal Statistical Society. Series B (Methodological)*, 26(2):211–252.

Crimmins, E. M., Johnston, M., Hayward, M., and Seeman, T. (2003). Age differences in allostatic load: an index of physiological dysregulation. *Experimental Gerontology*, 38(7):731–734.

Dublin, L. I., Lotka, A. J., and Spiegelman, M. (1949). *Length of Life*. Ronald New York.

Govorun, M., Jones, B. L., Liu, X., and Stanford, D. A. (2018). Physiological age, health costs, and their interrelation. *North American Actuarial Journal*, 22(3):323–340.

Herskind, A. M., McGue, M., Holm, N. V., Sörensen, T. I., Harvald, B., and Vaupel, J. W. (1995). The heritability of human longevity: a population-based study of 2872 danish twin pairs born 1870–1900. *Human Genetics*, 97(3):319–323.

Jones, H. B. (1956). A special consideration of the aging process, disease, and life expectancy. *Advances in Biological and Medical Physics*, 4:281–337.

Le Bras, H. (1976). Lois de mortalité et age limite. *Population*, 31(3):655–692.

Lin, X. S. and Liu, X. (2007). Markov aging process and phase-type law of mortality. *North American Actuarial Journal*, 11(4):92–109.

Neuts, M. F. (1982). Explicit steady-state solutions to some elementary queueing models. *Operations Research*, 30(3):480–489.

Olshansky, S. J. and Carnes, B. E. (1997). Ever since Gompertz. *Demography*, 34(1):1–15.

Slud, E. V. and Suntornchost, J. (2014). Parametric survival densities from phase-type models. *Lifetime Data Analysis*, 20(3):459–480.

Su, S. and Sherris, M. (2012). Heterogeneity of australian population mortality and implications for a viable life annuity market. *Insurance: Mathematics and Economics*, 51(2):322–332.

Szilard, L. (1959). On the nature of the aging process. *Proceedings of the National Academy of Sciences*, 45(1):30–45.

Yashin, A. I., Arbeev, K. G., Ukraintseva, S. V., Akushevich, I., and Kulminski, A. (2012). Patterns of aging-related changes on the way to 100. *North American Actuarial Journal*, 16(4):403–433.

Yashin, A. I., Vaupel, J. W., and Iachine, I. A. (1994). A duality in aging: the equivalence of mortality models based on radically different concepts. *Mechanisms of Ageing and Development*, 74(1-2):1–14.

About The Society of Actuaries

With roots dating back to 1889, the Society of Actuaries (SOA) is the world's largest actuarial professional organization with more than 31,000 members. Through research and education, the SOA's mission is to advance actuarial knowledge and to enhance the ability of actuaries to provide expert advice and relevant solutions for financial, business and societal challenges. The SOA's vision is for actuaries to be the leading professionals in the measurement and management of risk.

The SOA supports actuaries and advances knowledge through research and education. As part of its work, the SOA seeks to inform public policy development and public understanding through research. The SOA aspires to be a trusted source of objective, data-driven research and analysis with an actuarial perspective for its members, industry, policymakers and the public. This distinct perspective comes from the SOA as an association of actuaries, who have a rigorous formal education and direct experience as practitioners as they perform applied research. The SOA also welcomes the opportunity to partner with other organizations in our work where appropriate.

The SOA has a history of working with public policymakers and regulators in developing historical experience studies and projection techniques as well as individual reports on health care, retirement and other topics. The SOA's research is intended to aid the work of policymakers and regulators and follow certain core principles:

Objectivity: The SOA's research informs and provides analysis that can be relied upon by other individuals or organizations involved in public policy discussions. The SOA does not take advocacy positions or lobby specific policy proposals.

Quality: The SOA aspires to the highest ethical and quality standards in all of its research and analysis. Our research process is overseen by experienced actuaries and nonactuaries from a range of industry sectors and organizations. A rigorous peer-review process ensures the quality and integrity of our work.

Relevance: The SOA provides timely research on public policy issues. Our research advances actuarial knowledge while providing critical insights on key policy issues, and thereby provides value to stakeholders and decision makers.

Quantification: The SOA leverages the diverse skill sets of actuaries to provide research and findings that are driven by the best available data and methods. Actuaries use detailed modeling to analyze financial risk and provide distinct insight and quantification. Further, actuarial standards require transparency and the disclosure of the assumptions and analytic approach underlying the work.

Society of Actuaries
475 N. Martingale Road, Suite 600
Schaumburg, Illinois 60173
www.SOA.org